The Ocean's Response to a CO_2-Induced Warming

KIRK BRYAN AND MICHAEL J. SPELMAN

Geophysical Fluid Dynamics Laboratory/NOAA, Princeton University, New Jersey

The climate response to a large increase in atmospheric CO_2 was investigated in a numerical experiment with a coupled ocean-atmosphere model. The study is focused on one aspect of the experiment, the predicted response of the ocean to the warming episode. A fourfold increase in atmospheric CO_2 causes a warming sufficiently intense to produce a partial collapse of the thermohaline circulation of the ocean. Surprisingly, the wind-driven circulation of the ocean is maintained without appreciable change. The global hydrological cycle intensifies without a major shift of the pattern of net precipitation over the model ocean. In the warming episode the downward pathways for heat, which include diffusion and Ekman pumping, remain open. The partial collapse of the thermohaline circulation closes the normal upward pathways associated with abyssal upwelling and high-latitude convection. As a result the thermocline is able to sequester almost twice as much heat than would be predicted from the behavior of a neutrally buoyant tracer introduced at the surface under normal climatic conditions. An enhanced sequestering of heat would produce a negative feedback for greenhouse warming. However, the partial collapse of the thermohaline circulation found in the numerical experiment would also affect the global carbon cycle, possibly producing a climatic feedback as strong as that caused by an enhanced uptake of heat from the atmosphere.

1. INTRODUCTION

Bryan et al. [1982] and *Spelman and Manabe* [1984] reported on the transient behavior of a coupled ocean-atmosphere climate model abruptly perturbed by a fourfold increase in atmospheric CO_2. The degree of vertical mixing of an ocean heat anomaly is crucial in determining the effectiveness of the ocean as a climate buffer. If heat introduced at the surface were mixed uniformly throughout the entire volume of the ocean, the buffering effect of the ocean would be extremely great, and climate warming caused by anthropogenic increases of atmospheric CO_2 would be delayed for a century or more. However, studies of transient tracers suggest that it is more likely that a small heat anomaly introduced by a CO_2/climate change will be largely trapped above the main ocean thermocline. The model results for a coupled ocean-atmosphere system of *Bryan et al.* [1982] are consistent with this idea. An important conclusion of the coupled ocean-atmosphere study related to the pattern of transient response with respect to latitude. The transient response of sea surface temperature was normalized by the total response expected in a final equilibrium state with increased atmospheric CO_2. Only 10 years after "switch on" of high CO_2 the normalized response became rather uniform at all latitudes, indicating that the results of CO_2 climate sensitivity experiments provide useful information on the geographical pattern of the transient climate as long as the increase of anthropogenic CO_2 does not greatly exceed its present rate.

Geochemists [*Oeschger et al.*, 1975] have attempted to fit ocean transient tracer measurements by a simple one-dimensional model in which the ocean is represented as a mixed layer underlain by a diffusive thermocline. While a one-dimensional model captures some aspects of the transient tracer behavior, the actual processes by which tracers penetrate into the thermocline and the deep ocean are much more complex. *Sarmiento* [1983] has applied a three-dimensional model to the transient tracer problem, using the North Atlantic tritium data set for verification. While the ocean component of the climate model of *Bryan et al.* [1982] is less detailed in its horizontal resolution than that used by Sarmiento, it is based on the same formulation and has nearly the same vertical resolution. In a related study, *Spelman and Manabe* [1984] have analyzed the effect of ocean heat transport in the same coupled model on the overall climate sensitivity to increased CO_2. In this study we are concerned with the transient response and the details of the actual penetration of the heat anomaly into the ocean model. *Cess and Goldenberg* [1981] and *Hansen et al.* [1984] have assumed that the penetration of transient tracers can be used as a physical analogue for the penetration of a CO_2-induced heat anomaly. The transient tracers are purely passive, while a heat anomaly will change the buoyancy field. *Bryan et al.* [1984] found that a positive warm surface anomaly of only 0.5°C imposed on a model of the World Ocean behaved much like a passive tracer. In a recent study with a fully coupled model, *Schlesinger et al.* [1985] found that the ocean response to a doubling of atmospheric CO_2 also appeared to be consistent with transient tracer data. Based on an analysis of the coupled model experiment of *Bryan et al.* [1982], we attempt to determine if the tracer analogue still holds for larger perturbations caused by a fourfold increase in atmospheric CO_2.

While the present study concentrates on the effect of atmospheric CO_2 on climate, it is recognized that other greenhouse gases produced as the result of human activity are significant [*Hansen et al.*, 1984]. This makes the study of the climate response to changes of greenhouse gases even more important.

2. THE MODEL

Both the atmospheric and oceanic components of the model have been described in some detail in previous studies, but in order to make the present paper reasonably self contained, a very brief description will be given here. The coupled models contain a relatively detailed specification of the physical processes in climate in order to illustrate as many significant feedbacks as possible. The major simplifications involve the geometry of continent and ocean. The geometry of the model is bound to influence quantitative aspects of the results, but at this point the first priority is to identify as many important physical processes in the climate response as possible. The
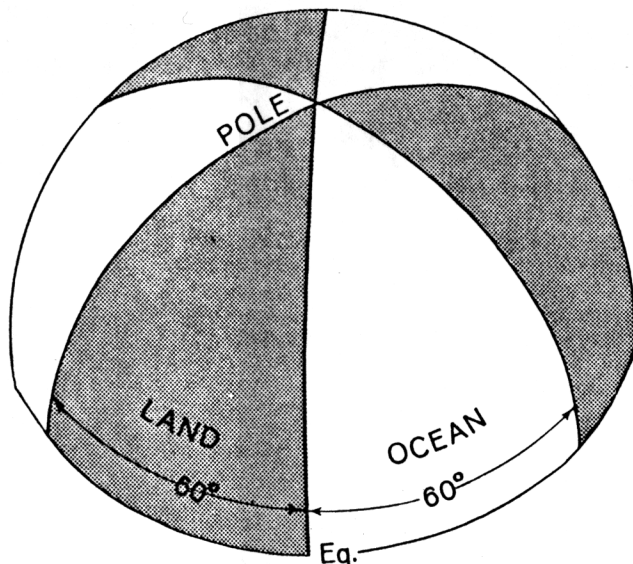
Fig. 1. Geometry of the coupled model [from *Spelman and Manabe*, 1984].

simplified geometry expedites both the calculations of the transient response, and the analysis of the final results.

The model is equivalent to a globe with three identical continents, 60° of longitude in the zonal direction, separated by three oceans of the same width. The atmosphere is constrained to be periodic over a 120° sector of longitude and mirror symmetry is imposed at the equator. The idealized geometry is shown in Figure 1. The atmospheric general circulation model contains a detailed specification of radiation, the hydrologic cycle, and the dynamics of synoptic disturbances. Except for this simplified geometry, it is essentially the atmospheric model used by *Manabe and Stouffer* [1980]. The ocean model and specification of pack ice is like that of *Bryan et al.* [1975]. The vertical resolution of the ocean model is enough to provide a good description of the thermocline, and the thermohaline circulation. It should be noted, however, that mirror symmetry across the equator excludes cross-equatorial cells in the thermohaline circulation. The horizontal resolution of approximately 4.5° latitude by 3.8° longitude is only marginally adequate for resolving the intense coastal currents, and mesoscale eddies in the ocean are only included implicitly through lateral mixing. The inclusion of salinity and a detailed equation of state for seawater allows for an interaction between the atmospheric hydrological cycle and the ocean circulation, which is quite important in polar latitudes.

The diagram in Figure 2 shows the experimental procedure. Equilibrium climate solutions are first established for normal atmospheric CO_2 and 4 times the normal atmospheric CO_2. The method used to reach equilibrium is outlined in *Manabe and Bryan* [1969] and *Bryan* [1984]. To test equilibrium, a numerical integration of 50 years duration is made by using the normal CO_2 climate solution as an initial condition for the coupled model. Globally averaged changes in heat content of the ocean during this control run amounted to less than 1 W/m^2 over the 50-year period, and the rms changes over any 5-year period amounted to less than 2 W/m^2 [*Bryan*, 1984]. In the control run a passive tracer is released at the surface of the model ocean and allowed to penetrate downward into the thermocline. In a second integration the transient response of climate to increasing CO_2 is tested in a "switch on" case in

which the atmospheric CO_2 is impulsively increased to 4 times its normal value.

Aside from the geometry, there are several other important simplifications that should be noted. The land surface lacks any topography, allowing the atmospheric flow to be much more zonal than it would be otherwise. Seasonal changes in radiation are not taken into account, and cloudiness is fixed by using climatological data. It should be noted that the importance of feedback connected with variable cloudiness has been emphasized by *Hansen et al.* [1984] on the basis of similar model calculations.

3. DESCRIPTION OF THE NORMAL CO_2 EQUILIBRIUM STATE

Before describing the response of the model to a sudden increase of CO_2, we will briefly describe the initial state. Surface currents, temperature, and salinity fields are shown in Figure 3(*a–c*). It is very important to include temperature and salinity separately in a climate model because these two fields respond in quite different ways to climate variations. The surface velocity field is helpful in understanding the temperature and salinity fields. There is a pronounced subtropical gyre centered at 25°N with a strong western boundary current. The eastward drift along the northern edge of the subtropical gyre splits into poleward and equatorward branches at the eastern boundary. In analogy with the North Atlantic the poleward branch is equivalent to the Norwegian Current, and the equatorward branch is equivalent to the Canary Current. The coarse horizontal grid of the model only allows rather weak currents, and the maximum velocity in the western boundary current does not exceed 30 cm/s.

The surface temperature is predominantly a function of latitude. A significant east-west gradient is only seen in the tropics of the model where a pool of warm water is located at the western boundary. Comparing with observations for the North Atlantic in Figure 4 we see that the model temperature pattern lacks the intense gradients associated with the Gulf Stream. Much more structure is shown in the salinity field. There are two reasons for this difference. One, the salinity at the surface has no direct feedback on the evaporation minus precipitation at the surface, while the temperature does affect the surface heat flux. Two, the salinity at the surface at most latitudes plays a lesser role in determining the surface density. Thus the salinity is forced to act as a nearly passive tracer.

Note that the salinity has a maximum in the subtropical gyre where evaporation is highest. A weak minimum is located
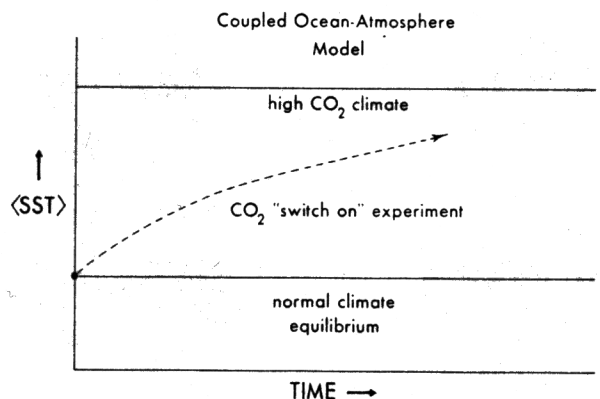

Fig. 2. A schematic diagram of the climatic response experiment with the coupled model. The ordinate is the globally averaged sea surface temperature. The two horizontal lines indicate normal and high CO_2 climate equilibria.
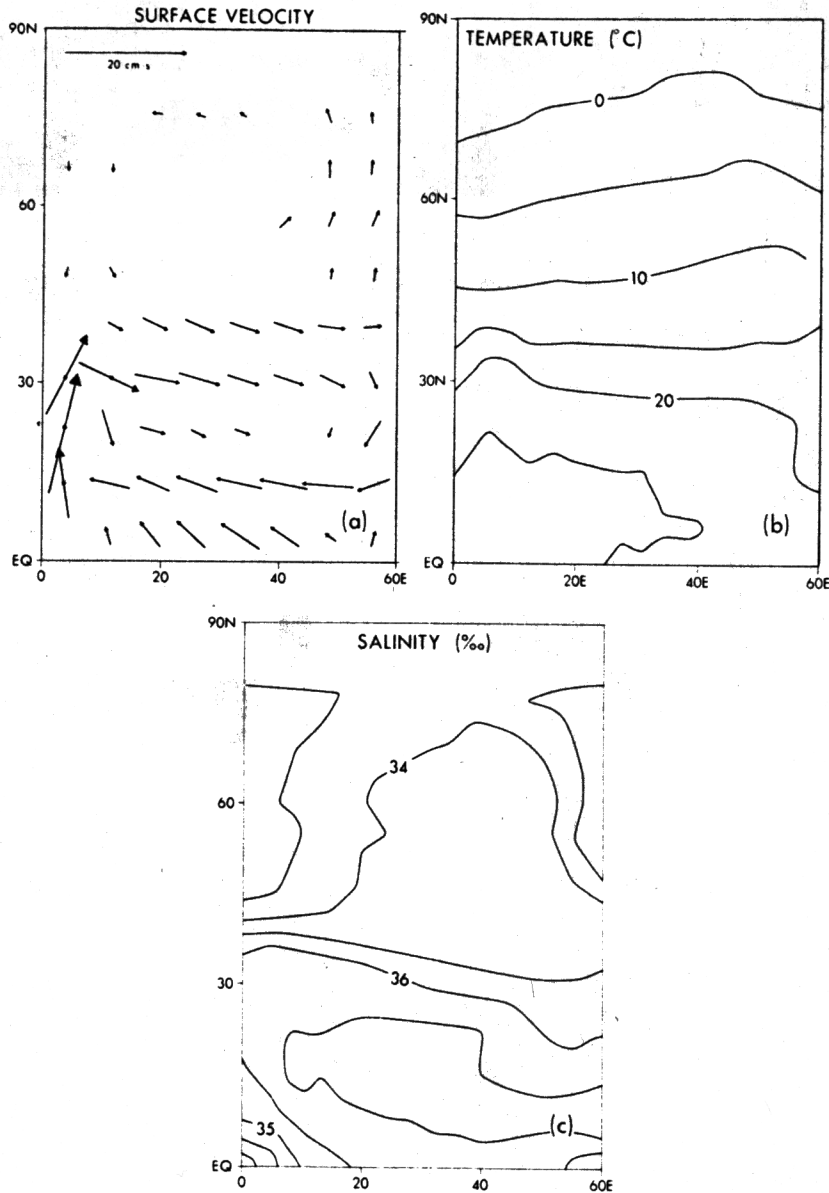
Fig. 3. (a) The surface velocity, (b) surface temperature (°C), and (c) surface salinity (‰) corresponding to the initial, normal CO_2 climate.

in the equatorial rainbelt. Runoff from land tends to produce minima on both sides of the model ocean between 50°N and 60°N. A long tongue of higher salinity extends along the poleward branch of the subarctic gyre. Most of these features have counterparts in the observed pattern of the North Atlantic shown in Figure 4. It is remarkable that the coupled model does such a good job in predicting the amplitude of salinity variations.

The vertical structure is shown in Figure 5(a, b), which allows a comparison of the zonally averaged temperature and
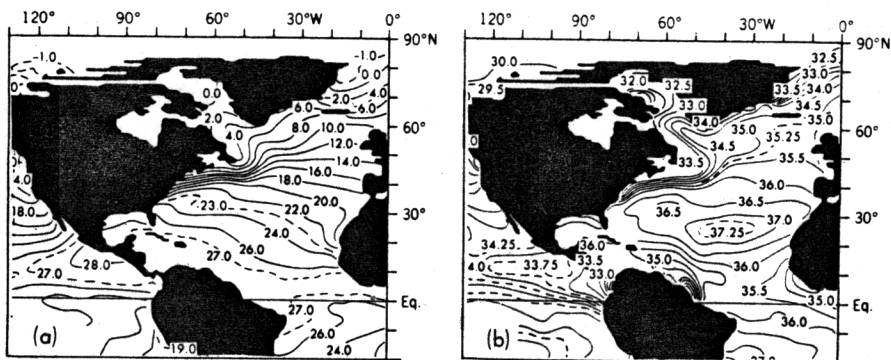

Fig. 4. Annual mean (a) temperature (°C) and (b) salinity (‰) in the North Atlantic from *Levitus* [1982].
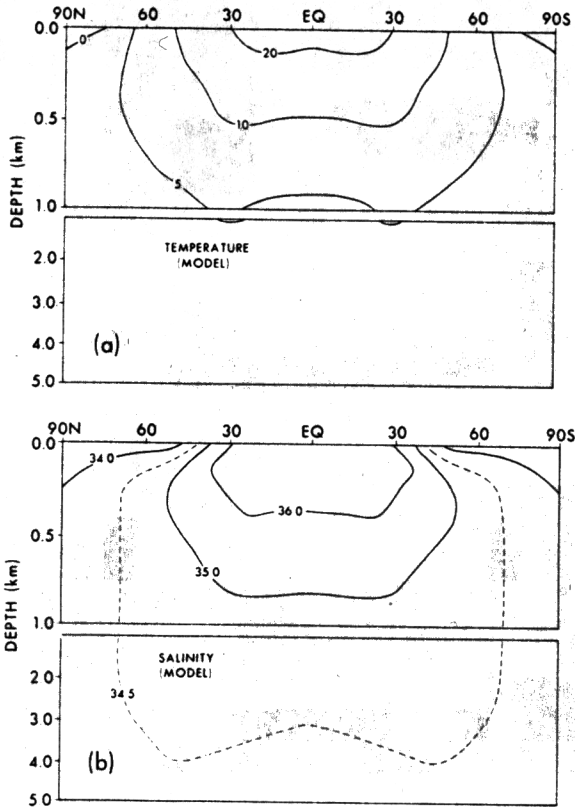
Fig. 5. Zonally averaged (a) potential temperature (°C) and (b) salinity (‰) from the model. Note that calculations are only done for one hemisphere.

surface warming of the ocean because of the shielding effect of the arctic halocline. Penetration of the heat anomaly into the ocean is pronounced in the subarctic, where the stratification is weakest. Penetration of the surface heat anomaly is relatively weak in low latitudes.

The surface wind stress and moisture flux averaged over the years 21–25 after "switch on" are shown in Table 1. Note that the changes in zonally averaged wind stress are, in most cases, less than 10%. This is a rather unexpected feature of the solution and is extremely important in determining the response of the model ocean to CO_2-induced warming. Somewhat more significant changes take place in the net moisture flux, which includes runoff from the adjacent land areas. As expected, climate warming results in an intensification of the global hydrological cycle. The zonally averaged values of precipitation minus evaporation plus runoff reflect an intensification of about 20%, with very little changes in the profile with respect to latitude. We will examine some of the changes in salinity that result from the intensification of the hydrological cycle and transient changes in ocean circulation at the end of this section.

The time history of a surface of constant density is shown in Figure 8. The four panels correspond to 0, 5, 15, and 20 years after "switch on," the time at which atmospheric CO_2 is impulsively increased to 4 times its normal value. Note that the surface is initially about 300 m deep in the subtropical gyre region, and there is an extensive area poleward of the outcrop of the density surface. After "switch on," this outcrop area rapidly shrinks. Decrease of surface density is particularly rapid near the pole. By year 15, much of the surface of constant density north of 40°N is below 200 m. In the panel corresponding to year 20 the outcrop area is very small. There

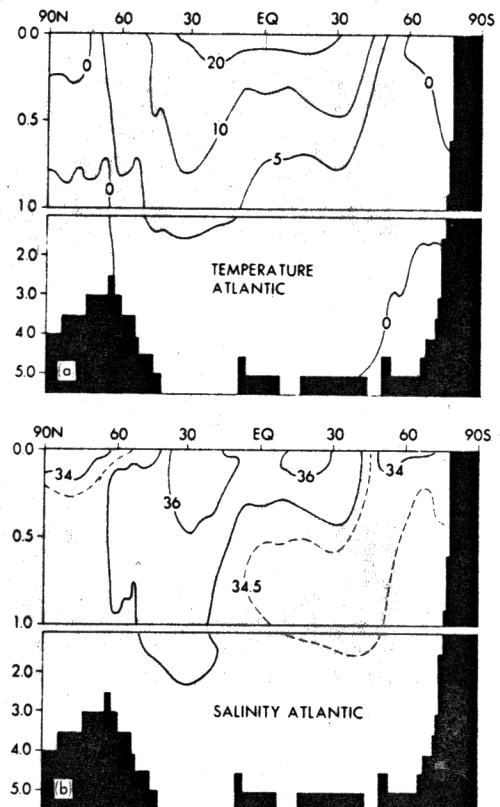salinity cross sections with those observed in the North Atlantic. In making a comparison we must keep in mind that the Atlantic thermohaline circulation is quite asymmetric across the equator, while the present model is forced to be symmetric. The maximum depth of the 10° isotherm at about 30°N is slightly less than 600 m. This is less than the observed depth of 800 m indicated in the North Atlantic (see Figure 6a). The 5° isotherm penetrates to about the same level. The model lacks the sharp up-bowing of isotherms near the equator, as shown in the observed pattern. The coarse resolution of the model does not provide a good simulation for the equatorial thermocline. Note the formation of a halocline in the polar region of the model. The ice that forms in this region is surrounded by a freshwater layer that shields warmer water below. The polar halocline plays a very important role in the transient response to CO_2-induced warming.

4. TRANSIENT RESPONSE TO A SUDDEN INCREASE OF ATMOSPHERIC CO_2

The previous section contained a description of the ocean circulation corresponding to the climate equilibrium of the coupled model for a normal atmospheric CO_2 content. We will now consider the transient response to a sudden quadrupling of atmospheric CO_2. To provide a concise picture of the response in both the atmospheric and ocean component of the model, we have included Figure 7, which is from *Spelman and Manabe* [1984, Figure 16a]. This figure shows the zonally averaged anomaly in the atmosphere and ocean 25 years after "switch on." Note that the atmospheric warming is most intense near the pole and at the surface. In the stratosphere the CO_2 loading actually leads to a cooling. The extreme warming of the atmosphere near the pole does not lead to an extreme

Fig. 6. Observed zonally averaged potential temperature (°C) and salinity (‰) for the Atlantic [*Levitus*, 1982].
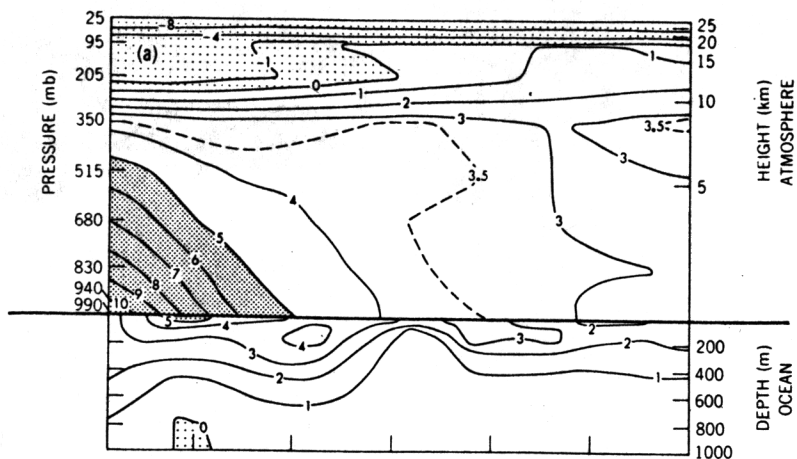
Fig. 7. The zonally averaged temperature change 25 years after "switch on" from *Spelman and Manabe* [1984].

are now two separate domes in the area poleward of 40°N. One contains the outcrop region and the other extends upward to within 100 m of the surface. The surface current pattern corresponding to year 20 is shown in Figure 9. Comparing it to the initial pattern in Figure 3a, we see some pronounced changes in the subarctic gyre. There are now two cyclonic gyres associated with the two domes shown in Figure 8 at 20 years. The tendency for the single cyclonic subarctic gyre to split into two cyclonic gyres as warming proceeds is an important feature of the transient response.

Slightly different information is conveyed by the time history of a deeper isopycnal surface shown in Figure 10. At year 5 the area of outcrop is already very small. By year 20 the area of outcrop has disappeared completely, and the dome between 40°N and 50°N dominates the displacement pattern. The contrast between the pattern of displacement before and after substantial warming has taken place is striking and demonstrates the very great importance of localized convection on the topography of isopycnal surfaces.

A penetration depth d of some variable μ may be defined as

$$d = \frac{1}{\mu_s} \int_{-H}^{0} \mu \, dz \qquad (1)$$

where μ_s is the surface value of μ and H is the total depth. The penetration depth averaged over the whole basin provides an integral measure of how much material introduced at the sur-

face of the ocean has been incorporated in the ocean itself. On the basis of a one-dimensional diffusive model one would expect that a warm anomaly would penetrate the ocean less efficiently than a passive tracer, since the warm anomaly would stabilize the upper ocean and inhibit downward mixing. An argument of this kind has been advanced in a recent study by *Harvey and Schneider* [1985], which examines climate response in terms of one-dimensional coupled atmosphere-ocean models.

In the present case a warm anomaly actually penetrates faster than one would expect from a passive tracer, indicating

TABLE 1. Zonally Averaged Eastward Component of the Wind Stress and Surface Moisture Flux Over the Model Ocean

Latitude	Wind Stress, dyn/cm^2		Moisture Flux, m/yr	
	Year 0	Years 21–25	Year 0	Years 21–25
84.4°	−0.23	−0.14	0.03	0.09
73.3°	−0.01	−0.02	0.60	0.69
64.4°	−0.02	−0.02	0.41	0.47
55.5°	−0.18	0.03	0.76	0.98
46.7°	0.34	0.40	0.63	0.63
37.8°	0.67	0.62	0.28	0.28
28.9°	0.31	0.29	−0.22	−0.28
20.0°	−0.18	−0.20	−0.95	−1.20
11.1°	−0.31	−0.33	−1.01	−1.26
2.2°	−0.13	−0.11	0.19	0.31

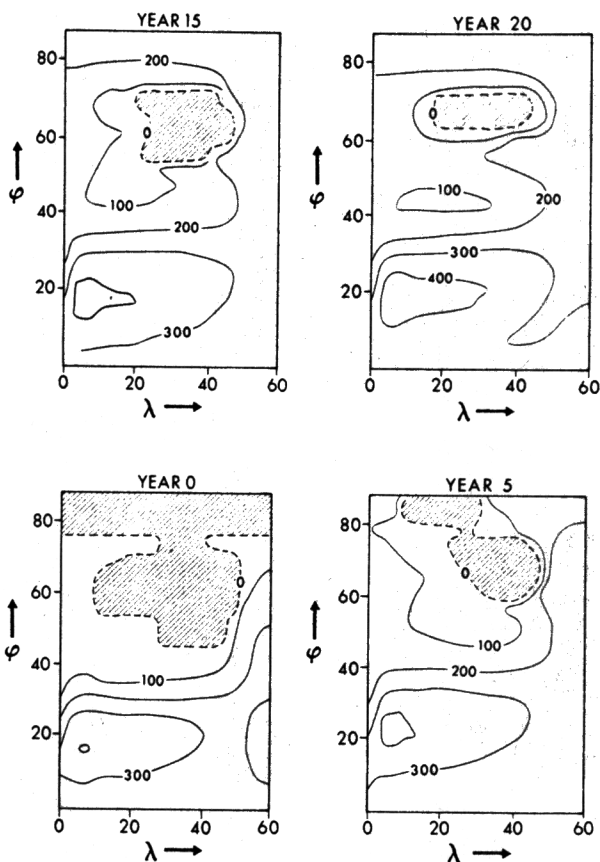Year 0 represents the initial condition; years 21–25 are after "switch on."

Fig. 8. The time history of displacement of the isopycnal surface, corresponding to $\sigma_\theta = 26.7$. Outcropping is shown by a dashed line. Displacement is in meters.
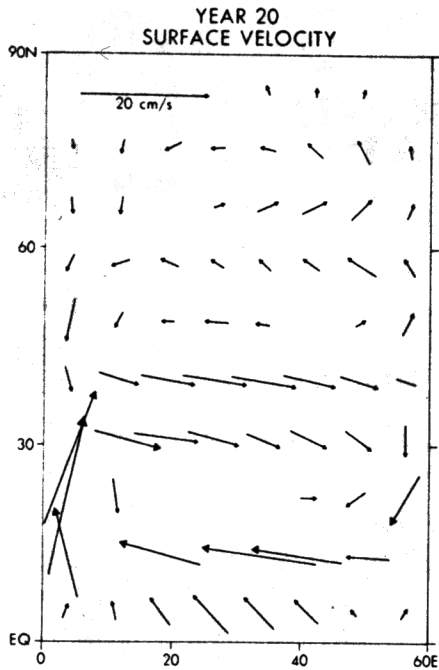
Fig. 9. The surface current pattern corresponding to year 20 after "switch on." Note the existence of two cyclonic gyres at high latitudes.
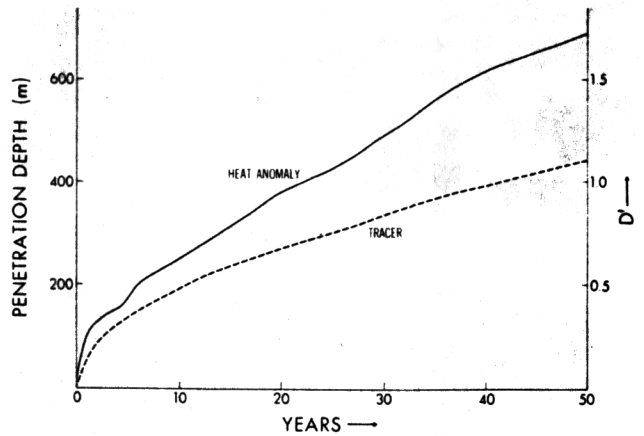

Fig. 11. The penetration depth in meters as defined by equation (1) as a function of time. The tracer experiment is done in the control case without surface warming. D' on the right is the penetration depth normalized by the scale depth of the pycnocline at year 0.

a feedback operating in the opposite direction. This behavior is demonstrated in Figure 11, which shows the penetration of a heat anomaly in the "switch on" case and the penetration of a passive tracer in the control run without any change in atmospheric CO_2. The figure shows that the passive tracer penetrates at about two thirds the rate of the heat anomaly. This behavior is somewhat counterintuitive. By way of explanation, Figure 12 is a schematic diagram of the heat balance of the ocean model. Under normal conditions, heat is introduced into the thermocline at low latitudes by ventilation and downward mixing. Ventilation is defined as the downward penetration of water along sloping isopycnals. Excess heat is carried poleward by ocean currents and then returned to the atmosphere by convection. In what follows we will show how this normal regime is disturbed when a large heating anomaly is introduced at the surface.

The equilibrium thermohaline circulation corresponding to normal and high (4 times normal) CO_2 is shown in Figure 13. The pattern of overturning in the meridional-vertical plane is similar to that found in previous model studies [see, for example, Bryan and Lewis, 1979]. The main feature is a large cell

with a concentrated downward branch at high latitudes and a broad upward branch that supports the main thermocline. In addition there are shallower cells near the surface that are associated with Ekman pumping and suction. The meridional circulation for high and normal atmospheric CO_2 is rather similar. The transient pattern shown in Figure 13b is dramatically different, however. This represents an average over the entire period of years 21–30. Water masses formed at high latitudes in the model in the warming episode do not have a high enough density to sink all the way to the bottom. Thus only intermediate water is formed, and deep water is bypassed. This leads to the formation of a new clockwise overturning cell in deep water. The main overturning cell of the normal thermohaline circulation has partially collapsed. As indicated in Table 1, zonal wind stresses do not diminish after "switch on." As a result the shallow cells near the surface caused by Ekman convergence are not changed significantly.

If one takes global averages over the entire ocean, horizontal heat transport and horizontal mixing are no longer significant, and vertical diffusion, vertical advection, and convection are the only transport processes remaining. Figure 14 shows the total fluxes by these processes in the control run and the "switch on" case. In the control run a near equilibrium exists so that the total surface flux is less than 1 W/m². A flux of this magnitude would be too small to detect from routine marine meteorological measurements. In the "switch on" case the heat uptake averaged over the period between 20 and 30 years is about 4 W/m². In Figure 15 the vertical heat flux is decomposed into those parts resulting from vertical diffusion, vertical advection, and convection. Diffusion must always carry heat
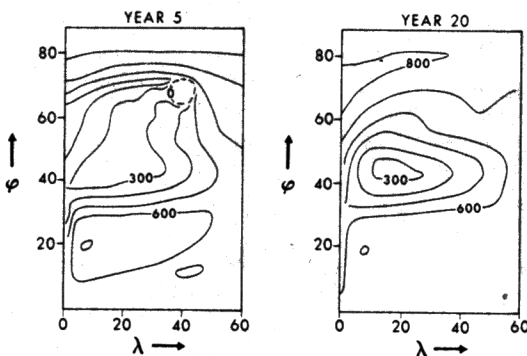

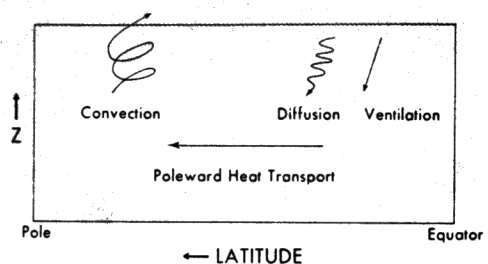Fig. 10. Same as Figure 8 for the $\sigma = 27.34$ surface.

Fig. 12. A schematic diagram of the heat balance of the model ocean. Ventilation is defined as the downward penetration of water along sloping isopycnals.
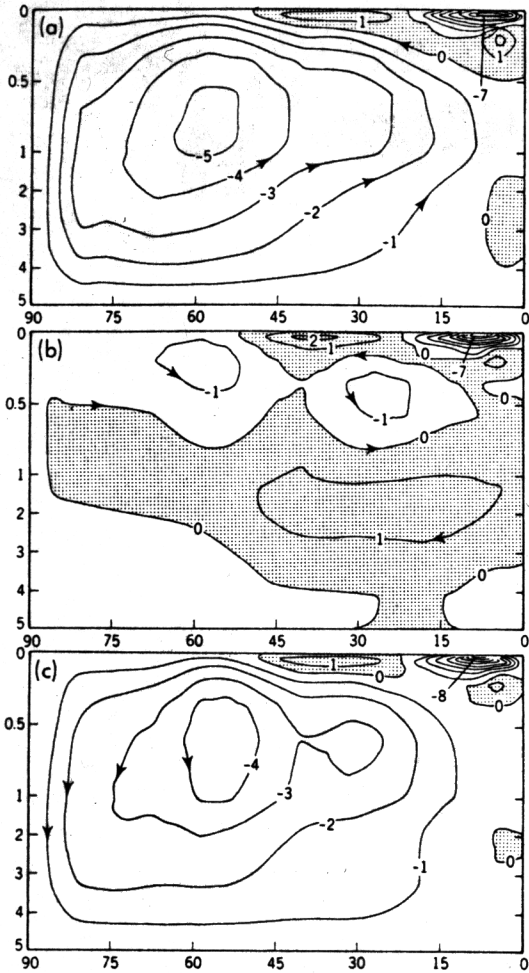
Fig. 13. The total meridional circulation in units of 10^{12} g/s: (a) equilibrium solution for high CO$_2$; (b) average circulation for years 21–30 after "switch on," showing the partial collapse of the thermocline; (c) equilibrium solution for normal CO$_2$. Note that the upper 1 km of ocean depth is expanded in the figure.

downward if temperature increases upward, and convection must always transport heat toward the surface unless salinity dominates the buoyancy field. Advection, however, can be of either sign. The vertical advection profile shown in Figure 15a is consistent with Figure 13c and the simple thermocline models of *Robinson and Stommel* [1959] and *Munk* [1966].
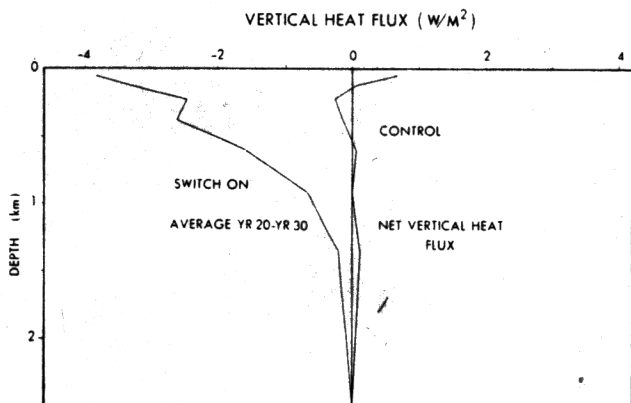

Fig. 14. Total vertical flux of heat for the control run and "switch on" case averaged over the entire ocean.
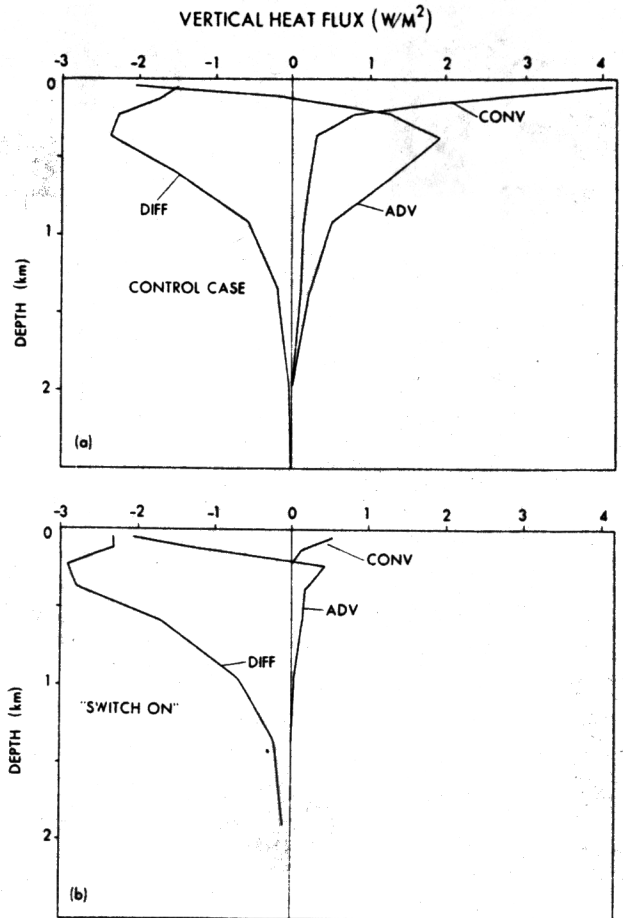

Fig. 15. The vertical flux decomposed into diffusion, convection, and vertical advection: (a) control run, (b) "switch on" case.

Wind-forced ventilation of the thermocline causes downward heat flux near the surface, while the thermohaline circulation induces an upward flux at the base of the thermocline.

In the control run, advection and diffusion both transport heat downward near the surface at a rate of about 2 W/m^2. This is balanced by an upward convective flux of about 4W/m^2. It must be recalled that these values are averages over the whole basin. Locally, convection could be more than an order of magnitude greater. In Figure 15b we see the vertical flux breakdown for the "switch on" case. Diffusion remains about the same as in the control case, since the vertical temperature structure has not been drastically modified at this stage. In the model, diffusivity is independent of the details of the stratification. Note that vertical advection at the base of the thermocline is greatly reduced because of a weakening of the thermohaline circulation. The wind-induced downwelling at the surface is still strong, however. The combined effect of diffusion and advection is therefore about 4 W/m^2, not very different from the control run. A drastic change, however, has taken place in convection as a result of warming of the ocean surface at high latitudes, which increases the vertical stability of surface waters. A decrease of surface salinity also plays an important role. In the absence of convection there is nothing to balance the downward flux of heat at lower latitudes, and the ocean gains heat more rapidly as the thermohaline circulation collapses and the thermocline moves downward.

In the introduction a question was raised regarding the analogy between the behavior of passive tracers and heat
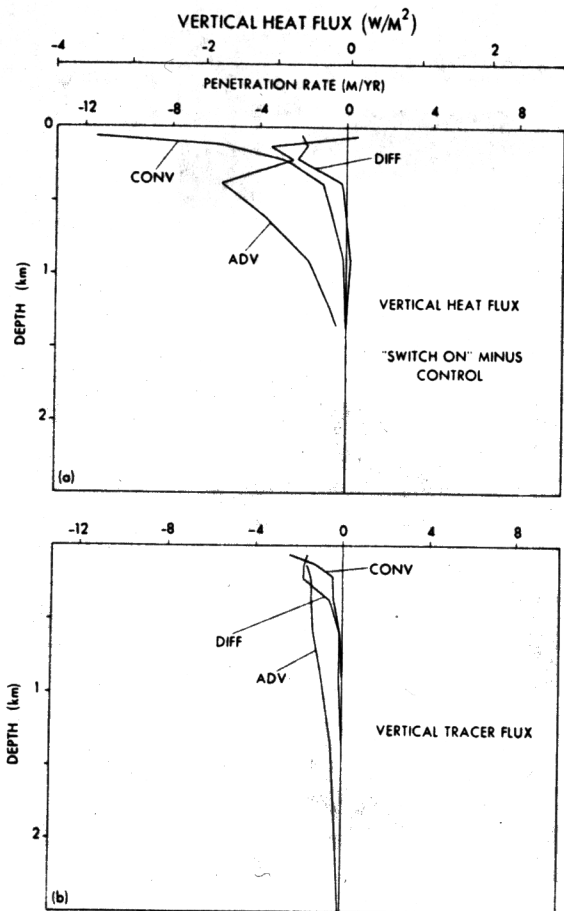
Fig. 16. (a) Components of the vertical heat flux averaged over the period 20–30 years minus the control run fluxes; (b) components of the vertical tracer flux.

anomalies. In Figure 16 we show the difference in vertical heat fluxes between the "switch on" and control runs. Subtracting the control run fluxes allows us to compare the anomalous fluxes with the fluxes for a passive tracer. Without feedback the heat flux minus the normal flux should be the same as the tracer fluxes. The fluxes are plotted in the same units by dividing by the surface value. This gives the rate of penetration. Note that the downward tracer flux is almost equipartitioned between diffusion, advection, and convection. In contrast the anomalous heat flux is dominated by the lack of convection in the "switch on" case. Near the surface, the contribution of the other terms is roughly the same in both cases. At depth the suppression of the thermohaline circulation, which normally supports the thermocline, allows a more rapid penetration.

The results in Figure 16 can be compared to the penetration depths shown as a function of time in Figure 11. The sum of the tracer fluxes at the surface corresponds to approximately 7 m/yr, while the anomalous heat fluxes at the surface corresponds to approximately 13 m/yr. In the 10-year period from 20 to 30 years after "switch on," Figure 11 shows that the tracer penetration depth increased 70 m and the heat anomaly penetration depth increased 120 m.

If we compare the salinity structure in the main thermocline for the equilibrium climates corresponding to high and normal CO_2 climates, we see marked differences. The zonally averaged salinity difference is shown in a cross section in Figure 17. Note that the surface waters become saltier in the subtropical gyre and fresher in polar latitudes as the climate

warms. At the equator itself the surface waters become slightly fresher. What we see is an intensification of the normal pattern brought about by a stronger hydrological cycle in the warm climate corresponding to high CO_2. Enhanced evaporation produces saltier surface water in the subtropics, and increased rainfall produces fresher water in polar regions.

The response of the surface salinity pattern 25 years after "switch on" can be seen by comparing Figure 18 with the equilibrium pattern shown in Figure 3c. Note that the pattern is generally the same, but the freshwater pools along the meridional boundaries at high latitudes have markedly intensified. This response is consistent with the net moisture flux increase at 55.5° latitude shown in Table 1. The salinity change in the latitude-vertical plane 25 years after "switch on," shown in Figure 19, indicates freshening at high latitudes and a weaker freshening in low latitudes. The transient salinity response can be explained by reversing the same arguments used for the heat anomaly. Fresh water is normally taken up by the oceans in polar latitudes and released in low latitudes, in contrast to heat. The sudden suppression of convection as a response to surface warming means that fresh water is trapped near the surface in high latitudes. The relaxation of the thermohaline circulation allows the surface waters at lower latitudes to freshen as salinity is diffused downward in the absence of normal abyssal upwelling.

5. DISCUSSION

In a previous study, *Bryan et al.* [1984] used a model of the World Ocean to test the response to surface anomalies. The model corresponded to that described by *Bryan and Lewis* [1979]. It was not coupled to an atmospheric model. Surface stress was simply specified from climatological data, and the flux of heat was set to be proportional to the difference between the surface temperature and a reference temperature. The flux of water resulting from evaporation minus precipitation was handled in the same way as the flux of heat. A warm anomaly was introduced at the surface by simply raising the reference temperature by 0.5°C globally. In a parallel experiment a tracer was imposed at the surface in a horizontally uniform way. The tracer and the positive temperature anomaly penetrated into the model ocean at approximately the same speed.
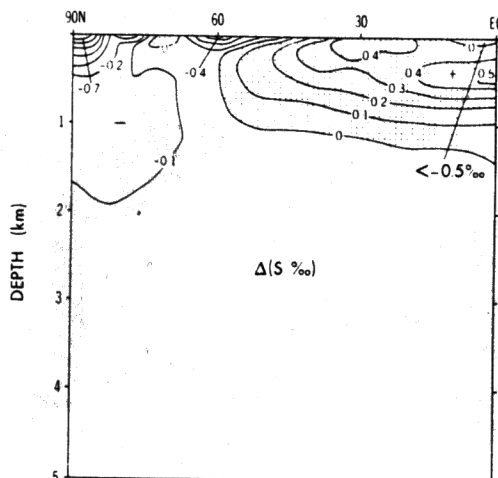

Fig. 17. The difference in zonally averaged salinity between the equilibrium climates corresponding to 4 times normal atmospheric CO_2 and normal atmospheric CO_2.

In the present study we are dealing with a much larger anomaly. Let us define the fractional response as the transient response normalized by the long-term response. At 20–30 years after "switch on" the fractional response of sea surface temperature is already 0.5–0.6 [*Spelman and Manabe*, 1984], and the total sensitivity of this model for 4 times normal CO_2 is over 4°C. Thus the effective positive surface temperature anomaly is nearly 4 times that considered by *Bryan et al.* [1984]. Therefore it is not surprising that the effects of buoyancy become more important in the present study. *Harvey and Schneider* [1985] have suggested that warming of the ocean surface could produce a positive feedback for CO_2-induced warming by impeding the diffusive penetration of heat into the upper ocean. The present model does not allow a full test of this idea because the vertical diffusivity is not a function of Richardson number and therefore independent of stability. On the other hand, our results suggest another feedback of opposite sign that potentially could be much stronger.

To understand the feedback caused by a large positive heat anomaly at the ocean surface the background heat balance of the model must be kept in mind. Under normal climate conditions, heat is received at the surface in low latitudes. It penetrates the main thermocline by ventilation and diffusion. The thermohaline circulation supports the thermocline by balancing this downward movement of heat and transporting heat to high latitudes. In high latitudes, convection carries heat upward to the surface, where it is lost to the atmosphere. A heat anomaly introduced at the surface interrupts this process. Convection is suppressed, and the thermohaline circulation can no longer support the thermocline. Thus the upward pathways of heat are blocked, while the downward pathways are still active. As a result the ocean's ability to sequester heat is greatly enhanced over what would be predicted from the same model for a neutrally buoyant tracer and a normal thermohaline circulation. In our calculations the enhancement leads to a doubling of the rate of penetration of a large heat anomaly.

For fresh water the opposite situation exists in the transient state. In the warming episode, downward pathways are blocked by the collapse of the thermohaline circulation, while upward pathways (Ekman pumping and diffusion) are still
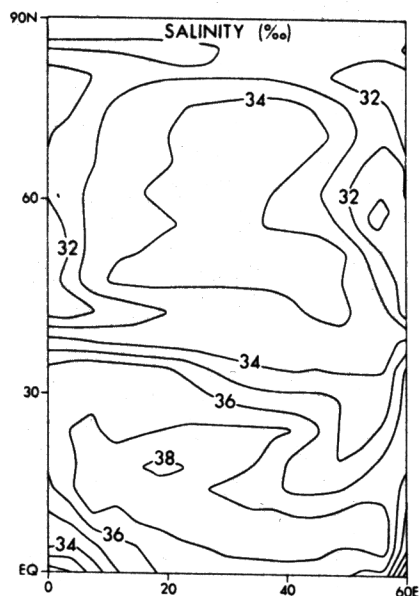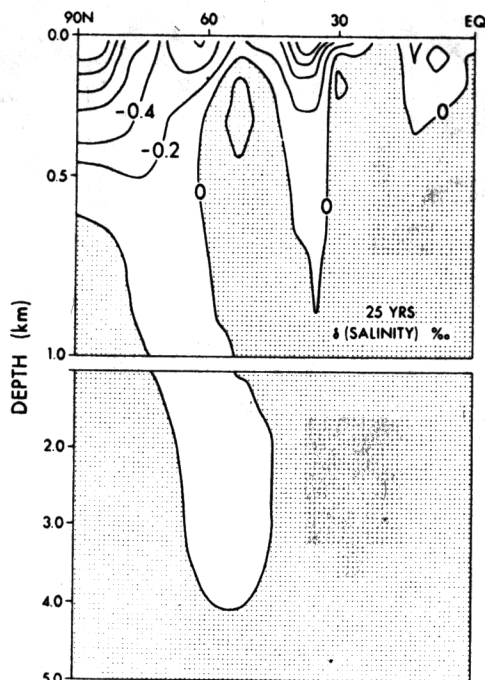
Fig. 19. Zonally averaged change in salinity 25 years after "switch on." Note that the surface salinity has decreased at nearly all latitudes.

open. As a result, center of mass of salinity in the ocean moves downward.

This numerical experiment reported in *Bryan et al.* [1982] and *Spelman and Manabe* [1984] must be judged as a first attempt to include an ocean circulation model in a study of climate response to a greenhouse warming. In the interpretation of the results, several caveats must be kept in mind. The heat anomaly considered is very large compared to any heat anomaly that could be caused by actual greenhouse gases in the forseeable future (25–50 years). Second, our one hemisphere idealized ocean is an extremely simple model of the World Ocean, and this restriction should be removed in future research. Finally, a partial collapse of the thermohaline circulation could have other far-reaching consequences outside the realm of the present model. For example, the suppression of water mass formation in the North Atlantic could decrease the ability of the ocean to take up CO_2. Another possibility suggested by the work of *Sarmiento and Toggweiler* [1984] is that sequestering of CO_2 by biological processes in high latitudes could actually be enhanced by a more sluggish thermohaline circulation. Uncertainties abound concerning the interaction of the ocean circulation and the carbon cycle. The carbon cycle and models for other greenhouse gases will have to be included in any complete prediction of the climate response to anthropogenic alteration of the earth's atmosphere.

REFERENCES

Bryan, K., Accelerating the convergence to equilibrium of ocean-climate models, *J. Phys. Oceanogr.*, *14*, 666–673, 1984.

Bryan, K., and L. J. Lewis, A water mass model of the World Ocean, *J. Geophys. Res.*, *84(C5)*, 2503–2517, 1979.

Bryan, K., S. Manabe, and R. L. Pacanowski, A global ocean-atmosphere model, Part 2, The oceanic circulation, *J. Phys. Oceanogr.*, *5*, 30–46, 1975.

Bryan, K., F. G. Komro, S. Manabe, and M. J. Spelman, Transient climate response to increasing atmospheric carbon dioxide, *Science*, *215*, 56–58, 1982.

Bryan, K., F. G. Komro, and C. Rooth, The ocean's transient response to global surface temperature anomalies, in *Climate Pro-*

Fig. 18. Surface salinity in the transient regime 25 years after "switch on." Compare this pattern with Figure 3c.

cesses and Climate Sensitivity, Geophys. Monogr., 29, Maurice Ewing Vol. 5, edited by J. E. Hansen and T. Takahashi, pp. 29–38, AGU, Washington, D. C., 1984.

Cess, R. D., and S. D. Goldenberg, The effect of ocean heat capacity upon global warming due to increased atmospheric carbon dioxide, J. Geophys. Res., 86, 498, 1981.

Hansen, J., A. Lacis, D. Rind, G. Russell, P. Stone, I. Fung, R. Ruedy, and J. Lerner, Climate sensitivity: Analysis of feedback mechanisms, Climate Processes and Climate Sensitivity, Geophys. Monogr. 29, Maurice Ewing Vol. 5, edited by J. E. Hansen and T. Takahashi, pp. 130–163, AGU, Washington, D. C., 1984.

Harvey, L. D. D., and S. H. Schneider, Transient climate response to external forcing on 10^0–10^4 year time scales, Part 1, J. Geophys. Res., 90(D1), 2191–2205, 1985.

Levitus, S., Climatological Atlas of the World Ocean, NOAA Publ. 13, 173 pp., U. S. Department of Commerce, Washington, D. C., 1982.

Manabe, S., and K. Bryan, Climate calculations with a combined ocean-atmosphere model, J. Atmos. Res., 26, 786–789, 1969.

Manabe, S., and R. Stouffer, Sensitivity of a global climate model to an increase of CO_2 concentration in the atmosphere, J. Geophys. Res., 85, 5529–5554, 1980.

Munk, W. H., Abyssal recipes, Deep Sea Res., 13, 707–730, 1966.

Oeschger, H., H. Siegenthalaer, U. Schotterer, and A. Gugelman, A box diffusion model to study the carbon dioxide exchange in nature, Tellus, 27, 168–192, 1975.

Robinson, A. R., and H. Stommel, The oceanic thermocline and the associated thermohaline circulation, Tellus, 11, 295–308, 1959.

Sarmiento, J. L., A simulation of bomb tritium entry into the Atlantic Ocean, J. Phys. Oceanogr., 13, 1924–1939, 1983.

Sarmiento, J. L., and J. R. Toggweiler, A new model for the role of the ocean in determining atmospheric P_{CO_2}, Nature, 621–624, 1984.

Schlesinger, M. E., W. L. Gates, Y.-J. Hau, The role of the ocean in CO_2-induced climate change: Preliminary results from the OSU coupled atmosphere-ocean general circulation model, in Coupled Ocean-Atmosphere Models, edited by J. C. Nihoul, Elsevier, New York, in press, 1985.

Spelman, M. J., and S. Manabe, Influence of oceanic heat transport upon the sensitivity of a model climate, J. Geophys. Res., 89, 571–586, 1984.

K. Bryan and M. J. Spelman, Geophysical Fluid Dynamics Laboratory/NOAA, Princeton University, P.O. Box 308, Princeton, NJ 08542.